Research article

Proposed cardio-pulmonary model to investigate the effects of COVID-19 on the cardiovascular system

R.T. Djoumessi, I.P. Dongmo Vougmo, J.S. Tadjonang Tegne, F.B. Pelap [*]

UR de Mécanique et de Modélisation des Systèmes Physiques (UR-2MSP), Faculté des Sciences, Université de Dschang, BP 69 Dschang, Cameroon

ARTICLE INFO

ABSTRACT

In this paper, we propose a new mathematical model of cardiovascular system coupled with a respiratory system to study the effects of COVID-19 on global blood circulation parameters using the lumped parameters model. We use the fourth-order Runge-Kutta method for solving the sets of equations of motion. We validate our model by showing that the simulated flows in pulmonary and aortic valves corroborate, respectively, the results established by Smith et al. [*IFAC Proceedings Volumes*, **39** (2006) 453–458]. Then we examine the effects of the new coronavirus (covid-19) on the cardiopulmonary system through the impact of the high respiratory frequency and the variation of the alveoli volume. To achieve this aim, we propose a new exponential law for the time varying of the pulmonary resistance. It appears that when the respiratory frequency grows, the delay between the systemic artery flow and the flow in the pulmonary artery diminishes. Therefore, the efficiency of the cardiac pump is reduced. Moreover, our results also show that variations of the alveoli volume cause the increment of the pleural pressure in the vascular cavities that induces an exponential growth of the pulmonary resistance. Furthermore, this growth of the pulmonary resistance provokes the augmentation of pressure in some organs and its reduction in others. We found that patient with covid-19 having a prior history of cardiovascular diseases is exposed to a severe case of inflammation/damage of certain organs than those with no history of cardiovascular disease.

1. Introduction

Clinical diagnosis and treatment decisions made by health workers could be improved by using mathematical models. Mathematical models play an important role in decision support. The heart is no exception; mathematical models have been developed to understand the electrical [9,35], mechanical [4,26] and electromechanical [18,28] behaviors as well as the blood flow [1,22] in this organ. These models highlight the dynamics of the heart and allow clinicians to better understand and plan their treatment. Let us note that when the heart is working, its dynamic is influenced by that of the other organs that collaborate with it. Indeed, the heart being housed in the rib cage, its behavior is influenced by the movements of the rib cage induced by the respiratory system which regulates the pressure of the rib cage. So to better understand the dynamics of the heart, it is important to produce a model that takes into account the respiratory system. For this purpose, several models have been developed in the literature, the most recent of which are cited by Refs. [12,16].

To the best of our knowledge, no such model has yet been studied to examine the case of COVID-19. In the literature, several models

---

have been proposed to study the cardiovascular system, and these models vary according to the parameters and organs to be modeled [2,36]. [27] proposed a left ventricle model coupled to systemic circulation to study ventricular circulation. This model, although complete, takes into account only one organ (left ventricle). To enlarge the system a little more, some authors [32] added to the previous model other elements such as the systemic and pulmonary circulation [32]. built a 6-compartment model with variable elastance which takes into account the left and right ventricles, the pulmonary vein, the systemic vein, the pulmonary artery. However, the model does not consider the opening and closing of the heart valves. Then [17], introduced an 8-compartments model to study the circulation in a normal and pathological situation. Although this complete model is capable of simulating certain pathologies, it does not take into account diastole and systole during its operation. Moreover [14], elaborated a cardiovascular system model for diagnosis. This model contains all the parameters necessary for systemic and pulmonary circulation.

However, not all of these models take into account the respiratory system. Most cardiopulmonary models do not take into account strong interaction between the pulmonary and cardiovascular (CVS) models. They are mainly either cardiovascular or pulmonary, with the exception of two models [24,25]. The model constructed by Ref. [24] integrates the important components of the cardiopulmonary system and highlights their interaction, in order to explore how this system responds to perturbations. The cardiac model used is based on the model of [5] and the respiratory model characterizes the resistance properties of the upper airways and the lungs. On the other hand, the Montebelli model [25] displayed cardiopulmonary interactions by simulating spontaneous breathing in healthy individuals and patients with chronic obstructive pulmonary disease.

Most recently, the coronavirus (COVID-19) pandemic affected the entire world. This disease is a pathology that attacks the respiratory system, swelling the respiratory alveoli that block the blood circulation. COVID-19 is caused by coronavirus-2, a severe acute respiratory syndrome, which invades cells via the angiotensin-2 converting enzyme receptor [15]. Research is conducted on this virus to try to understand its proliferation and attack scheme on the respiratory system. At the cellular level, some authors [7,15] showed that patients with cardiovascular disease are more vulnerable to this pathology. Among patients with COVID-19, the prevalence of cardiovascular disease is high, with more than 7% of patients experiencing myocardial injury as a result of infection 22% of severely ill patients [7]. Given the severity and aggressiveness of this disease on the cardiovascular system, our motivation in this paper is to propose a mathematical model of the cardiopulmonary system that will allow us to investigate the effects of COVID-19 on the heart and vascular circulation. To achieve this aim, we must answer the following question: *how to better understand the impact of this disease on patients with or without cardiovascular disease?*

In this paper, we propose a cardiopulmonary model that allows health care personnel to simulate the condition of a patient with COVID-19 by modifying parameters such as pulmonary artery pressure, pulmonary vein pressure and respiratory alveolar volume. The structure of this paper is organized as follows. In section II, we introduce a new model of cardio-respiratory system that includes significant parameters of COVID-19. Here, the mathematical model of each component of the system (i.e., cardiovascular system, ventricle mechanical model, pulmonary system) is suitably constructed and modified to include new considerations. Then, we couple the cardiovascular and respiratory systems to form the cardiopulmonary system and examine the effects of COVID-19 on it. In section III, we present the established results and corresponding discussions aiming to validate our mathematical model. We also modify some parameters of the respiratory system to simulate the state of patient with COVID-19. Concluding remarks are given in the last section.

2. Materials and methods

2.1. Cardiovascular system

In this section, we propose a 6-compartment model, describing the cardiovascular system. The system is composed of the pulmonary circulation (pulmonary artery (*Pa*), pulmonary veins (*Pv*)), the right and left ventricles (*rv* and *lv*), the systemic circulation
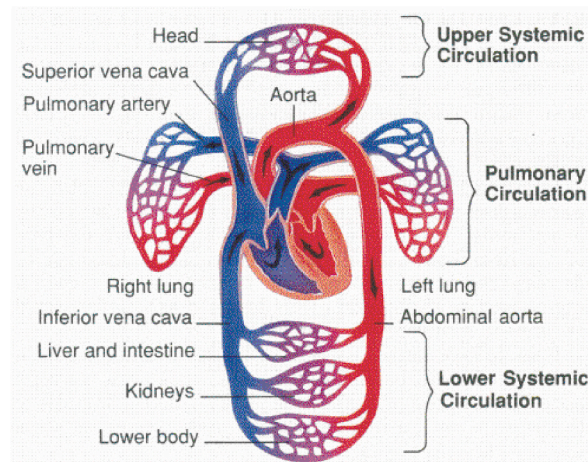

Fig. 1. Human cardiovascular system [32].

(systemic artery (*Sa*) and systemic vein (*Sv*)). The model presented is intended to simulate the essential haemo-dynamics of the cardiovascular system including the heart (Fig. 1).

We exploit the lumped parameter method [20] to construct the equations that govern the dynamics of the system. To reach this goal, we derive the analogous six-compartment model lumped parameter system depicted in Fig. 2.

Compartments analogy [37] was used for constructing our cardiovascular system model. With this approach, the cardiovascular system can be seen as series-connected of elastic compartments considered as a reservoir filled with blood. At any time, each compartment is characterized by the pressure $P(t)$ acting on the compartment walls, the volume $V(t)$ within it, the inlet $F_i(t)$ and outlet $F_o(t)$ flow rates. The scheme of the elastic chamber is drawn in Fig. 3.

According to the laws of the mass conservation, the equations describing the evolution of the volume in each elastic compartment can be written as follows:

$$\frac{dV_{lv}}{dt} = F_{i,l} - F_{o,l} \tag{1}$$

$$\frac{dV_{Sa}}{dt} = F_{0,l} - \frac{P_{Sa} - P_{Sv}}{R_s} \tag{2}$$

$$\frac{dV_{Sv}}{dt} = \frac{P_{Sa} - P_{Sv}}{R_s} - \frac{P_{Sv} - P_{rv}}{R_{tc}} \tag{3}$$

$$\frac{dV_{rv}}{dt} = F_{i,r} - F_{o,r} \tag{4}$$

$$\frac{dV_{Pa}}{dt} = F_{o,r} - \frac{P_{Pa} - P_{Pv}}{R_p} \tag{5}$$

$$\frac{dV_{Pv}}{dt} = \frac{P_{Pa} - P_{Pv}}{R_p} - \frac{P_{Pv} - P_{lv}}{R_{Pv}} \tag{6}$$

where $F_{o,r}$, $F_{o,l}$, $F_{i,r}$ and $F_{i,l}$ are the out flow from right and left ventricles, the flow inter the right and left ventricles, respectively. Here the subscripts r and l are the abbreviation of right and left. Within equations (1)–(1)–(6)(1)–(6), the diverse quantities can be found in Ref. [33] and are defined as:
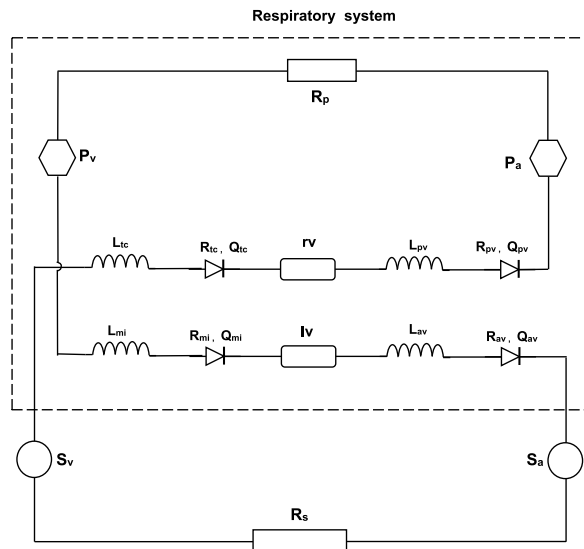

Fig. 2. Analogous lumped parameter system of cardio-pulmonary system, The system is made of pulmonary artery (Pa), pulmonary veins (Pv), right and left ventricles (rv and lv) systemic artery (Sa) and systemic vein (Sv). The parameters R_{mi}, R_{pv}, R_{tc} and R_{av} stand for the resistances of the mitral valve, the pulmonary valve, the tricuspid valve and the aortic valve, respectively. The factors L_{mi}, L_{tc}, L_{pv} and L_{av} designate, respectively, the inertia of the mitral valve, the tricuspid valve, the pulmonary valve and the aortic valve. The quantities Q_{mi}, Q_{pv}, Q_{tc} and Q_{av} are, respectively, the flow through the mitral valve, the pulmonary valve, the tricuspid valve and the aortic valve. The grandeurs R_p and R_s define the resistances of the pulmonary circulation and the systemic circulation, respectively. The organs in the interrupted area are in contact with the respiratory system.
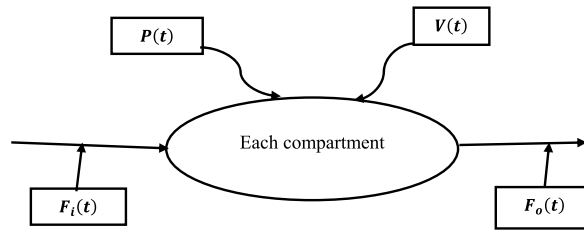
Fig. 3. Diagram of the elastic compartment of the cardiovascular system displaying the out flow $F_o(t)$, the inflow $F_i(t)$, the pressure $P(t)$ and the volume $V(t)$ of the elastic chamber.

$$F_{i,r} - F_{o,r} = \begin{cases} 0 & if \quad Q_{tc} < 0 \ and \ Q_{pv} < 0 \\ -Q_{pv} & if \quad Q_{pv} < 0 \\ Q_{tc} & if \quad Q_{pv} < 0 \\ Q_{tc} - Q_{pv} & otherwise \end{cases} \quad ; \quad F_{i,l} - F_{o,l} = \begin{cases} 0 & if \ Q_{mi} < 0 \ and \ Q_{av} < 0 \\ -Q_{av} & if \ Q_{mi} < 0 \\ Q_{mi} & if \ Q_{av} < 0 \\ Q_{mi} - Q_{av} & otherwise \end{cases}$$

$$\frac{dQ_{pv}}{dt} = \begin{cases} 0 & if \ P_{rv} \leq P_{pa} \\ \dfrac{P_{rv} - P_{pa} - Q_{pv}R_{pv}}{L_{pv}} & if \ P_{rv} > P_{pa} \end{cases} \quad ; \quad \frac{dQ_{tc}}{dt} = \begin{cases} 0 & if \quad P_{sv} \leq P_{rv} \\ \dfrac{P_{sv} - P_{rv} - Q_{tc}R_{tc}}{L_{tr}} & if \ P_{sv} > P_{rv} \end{cases}$$

$$\frac{dQ_{mi}}{dt} = \begin{cases} 0 & if \ P_{pv} \leq P_{lv} \\ \dfrac{P_{pv} - P_{lv} - Q_{mi}R_{mi}}{L_{mi}} & if \ P_{pv} > P_{lv}; \end{cases} \quad ; \quad \frac{dQ_{av}}{dt} = \begin{cases} 0 & if \ P_{lv} \leq P_{sa} \\ \dfrac{P_{lv} - P_{sa} - Q_{av}R_{av}}{L_{av}} & if \ P_{lv} \geq P_{sa} \end{cases}$$

in which the undefined quantities are clarified in the caption of Fig. 2. Furthermore, the parameters characterizing the vascular system in the non disease (basal) conditions are given in Table 1. In these equations, P_{pa}, P_{pv}, P_{sa}, P_{sv}, P_{lv} and P_{rv} are, respectively, the pressures in the pulmonary artery, the pulmonary vein, the systemic artery, the systemic vein, the left ventricle and the right ventricle. To avoid repetition, the other parameters and subscripts are defined in the caption of Fig. 2.

2.2. Ventricle mechanical models

According to Ref. [34]; we assume that the isometric pressure/volume function is exponential at the end of the diastole when the ventricle is relaxed and, linear at the end of the systole when the ventricle is maximally contracted. Then, the ventricular end-diastolic and end-systolic pressure-volume relationships could be written as:

$$P_{ED} = E(V_{ES} - V_0) \tag{7}$$

$$P_{ES} = B exp \lfloor A(V_{ED} - V_0) \rfloor - B \tag{8}$$

In Eqs. (7) and (8), the subscript ES refers to the end-systolic whereas the subscript ED stands for the end-diastolic; the parameter E designates the end-systolic elastance of the ventricle while V_0 represents the corresponding ventricle unstressed volume. The quantities B and A are coefficients describing the exponential shape of the end-diastolic pressure-volume relationship. By introducing the time varying ventricle activation function $0 < \varphi(t) < 1$ (with $\varphi(t) = 0$ at the maximum contraction and $\varphi(t) = 1$ at the complete relaxation) and assuming that $V_{lv} = V_{ES} = V_{ED}$ at the beginning of the cardiac cycle, the left ventricle is maximally contracted and we have:

$$P_{max,lv} = \varphi(t)P_{ED} + [1 - \varphi(t)]P_{ES} \tag{9}$$

By expanding Eq. (9), the dynamics of the left ventricle mechanical model will be described by:

$$P_{max,lv} = \varphi(t)E_{lv}(V_{lv} - V_{0.lv}) + (1 - \varphi(t))\{B_{lv} \ exp[A_{lv}(V_{lv} - V_{0.lv})] - B_{lv}\} \tag{10}$$

Through an analog investigation, similar expression to Eq. (10) that describes the dynamics of the right ventricle mechanical model

Table 1
Parameters characterizing the vascular system in the basal conditions (non disease conditions) [32].

Hydraulic Resistance ($Kpa.s.mL^{-1}$)		Inheritance ($Kpa.s^2.mL^{-1}$)
$R_p = 0.1552$	$R_{pv} = 0.0055$	$L_{mi} = 7.6968e - 5$
$R_s = 1.0889$	$R_{tc} = 0.0237$	$L_{av} = 1.2189e - 4$
$R_{av} = 0.0180$	$R_{mi} = 0.0158$	$L_{tc} = 8.0093e - 5$
		$L_{pv} = 1.4868e - 4$

could be deduced:

$$P_{max,rv} = \varphi(t)E_{rv}(V_{lv} - V_{0.rv}) + (1 - \varphi(t))\{B_{rv} \, exp[A_{rv}(V_{rv} - V_{0.rv})] - B_{rv}\} \qquad 11$$

Below are exposed all the parameters utilized for the simulations of the dynamics of the ventricle mechanical models (Table 2).

2.3. Pulmonary system

For the breathing generator, we use the Liénard system as the basis for modeling the breathing rhythm generator. Indeed, Liénard systems [12,23] consist of two-dimensional ordinary differential equations. The proposed model of the breathing generator is then defined by the following equations:

$$\begin{cases} \dfrac{dx}{dt} = (ay^2 - by)x + (ay^3 + by^2) - HB\dfrac{dV_{alv}}{dt} \\ \qquad \dfrac{dy}{dt} = x \end{cases} \qquad 12$$

where x represents a hidden variable, y defines the activity of the respiratory rhythm generator, V_{alv} designates the alveolar volume and HB is a constant. This constant refers to the Hering-Breuer reflex [6,19], triggered to prevent over-inflation of the lungs. In Eq. (12), the choice of a and b defines the form and the frequency (f_R) of the respiratory oscillations. Let us stress that the pressure inside the pericardium is given by the sum of the thoracic pressure P_{pl} and the intramural pericardial pressure P_{pcd}, that is:

$$P_{peri} = P_{pcd} + P_{pl} \qquad 13$$

In the presence of muscular activity, the thoracic pressure is computed as function of the rib cage volume V_{th} as:

$$P_{pl} = P_{mus} + E_{cw}(V_{th} - V_{tho}) \qquad 14$$

wherein E_{cw} and V_{tho} define the thoracic elastance and the unstressed rib cage volume, respectively. At this level, many scientists introduced several models of measuring the pressure generated by the muscle. Indeed [29], proposed a physiological model of this pressure nevertheless this model does not highlight the respiratory cycle. After what [10], introduced a sinusoidal model but their proposal was rather phenomenological and did not consider the slightest variations in frequency during breathing. In fact, the pressure generated by the respiratory muscle P_{mus} is the result of the conversion by the muscles of the respiratory pattern generator output into pressure. Therefore, the quantity P_{mus} is defined in our proposed model as an integral of the central respiratory activity y generated by the respiratory oscillator and disrupted by the alveolar volume. Then, the pressure generated by the respiratory muscle is given by:

$$\frac{dP_{mus}}{dt} = \lambda y + \mu \qquad 15$$

The parameter λ is a positive constant and allows the thoracic pressure P_{pl} to be set at physiological values. The factor μ compensates the leaks so as to keep a constant main value for the pressure.

Within Eq. (14), the rib cage volume V_{th} is evaluated as the sum of the intra-thoracic blood volume (V_{bth}) and the alveolar volume (V_{alv}), that is:

$$V_{th} = V_{bth} + V_{alv} \qquad 16$$

Therefore, the human mechanical respiratory system could be described by:

$$\frac{dV_{alv}}{dt} = -\frac{P_{pl} - E_{alv}V_{alv}}{R_{ua} + R_{ca}} \qquad 17$$

In relation (17), the factor E_{alv} defines the elastance of the alveolar, the parameter R_{ua} designates the resistance of the upper airways and R_{ca} stands for the resistance of the central airways. Therefore, the initial values of the respiratory variables are given in Table 3 while Table 4 displays the values of the various parameters of the respiratory system.

To summarize this section, let us mention that equations 12–17 describe the dynamics of the pulmonary system in which (12) simulates the respiratory rhythm while equations 13–17 describe, respectively, the dynamics of the thoracic pressure, the volume of rib cage, the respiratory muscle pressure and the alveoli volume. All these equations are coupled side by side as relations (12)-(12)-(17)

Table 2
Parameters of the ventricle mechanical models.

Left ventricle	Right ventricle
$E_{lv} = 2.95 mmHg/mL$	$E_{rv} = 1.75 mmHg/mL$
$V_{0.lv} = 16.77 mL$	$V_{0.rv} = 40.08 \, mL$
$B_{lv} = 1.5 mmHg$	$B_{rv} = 1.5 \, mmHg$
$A_{lv} = 0.014 mL^{-1}$	$A_{rv} = 0.011 mL^{-1}$
$K_{R.lv} = 0.000375 \, s/mL$	$K_{R.rv} = 0.0014 s/mL$

Table 3
Initial values of the state variables of the respiratory system [11].

Variables	Initial value
V_{alv}	0.51
P_{mus}	$0 cmH_2O$
x	-0.6
y	0

(12)-(17).

2.4. Design of the cardiopulmonary model

This section deals with the design of a comprehensible mathematical cardiopulmonary model that correctly describes the interactions of the cardiovascular system and the respiratory system. The relation between respiratory and circulatory system consists not only of their functional connection (i.e., in gas exchange), but naturally, also of their physical proximity inside the thorax. The interaction between these two models (cardiovascular system and respiratory system) could be materialized through the thoracic pressure (P_{pl}) and the intrathoracic volume (V_{bth}). Indeed, the thoracic pressure is used to compute the left and right ventricles pressure. This thoracic pressure should be taken into account during the respiration. Therefore, by exploiting Eqs. 10 and 11, the known expression of the thoracic pressure is modified as follows:

$$P_{lv} = P_{max,lv} - R_{lv}F_{o,l} + P_{peri} \qquad \text{18a}$$

$$P_{rv} = P_{max,rv} - R_{rv}F_{o,r} + P_{peri} \qquad \text{18b}$$

Within Eq. (18), the resistances of the left and right ventricles are given, respectively, by $R_{lv} = K_{R,lv}P_{max,lv}$ and $R_{rv} = K_{R,rv}P_{max,rv}$. The quantities $K_{R,lv}$ and $K_{R,lv}$ are constant parameters.

On the other hand, the volume of intra-thoracic blood (V_{bth}) is now defined as the sum of the pericardium blood volume (V_{pcd}), the pulmonary vein and artery blood volumes (V_{pu} and V_{pa}); all volumes calculated with the cardiovascular model. This volume corresponds to the volume that appears in the lung and can be computed with the cardiovascular system as:

$$V_{bth} = V_{pcd} + V_{pu} + V_{pa} \qquad \text{19}$$

In Eq. (19), the intramural pericardial pressure P_{pcd} is computed like [32]. For simulation measures, we homogenize all the units, especially the pressures which are all in K_{pa}, and express the time in seconds.

2.5. Effects of the new coronavirus on the cardiopulmonary system

When the coronavirus is received, it penetrates the mucous membranes of the nose, mouth, and eyes. Once the virus has entered a healthy cell, it uses them to make new virus parts. It multiplies and infects neighboring cells. For better understanding, let's try to imagine the respiratory tract as an upside-down tree whose trunk is a trachea or windpipe. It splits into smaller and smaller branches in the lungs. At the end of every neighboring are tiny air sacs known as alveoli. In each alveolus, oxygen enters the blood and carbon dioxide comes out.

After the infection, the coronavirus type II cells emit inflammatory signals that recruit macrophages (immune cells). These macrophages release cytokines that cause vaso-dilation which allows more immune cells to come to the site of injury and exit the capillary. As the results of this, the fluid accumulates in the alveolus (Fig. 4b and c) and this fluid dilutes the surfactant which triggers the onset of alveolar that collapse. The direct consequence of such action is the decrement of the gas exchange and the growth of the work of breathing by increasing the respiratory pattern. Furthermore, the fluid that fills the respiratory alveoli increases its volume until it ruptures due to the presence of immune cells in the cavity. Fig. 4a-c displays the evolution of the destruction of a respiratory alveolus [31]. As explained within their work, as Covid-19 multiplies, it infects neighboring cells which, when they die, accumulate in the respiratory alveoli. Due to the rapid proliferation of the virus, the respiratory alveoli are quickly overwhelmed and burst.

To model the impact of coronavirus in the cardiopulmonary system, we modify the rib cage volume V_{th} by introducing a parameter

Table 4
Various parameters of the respiratory system [11].

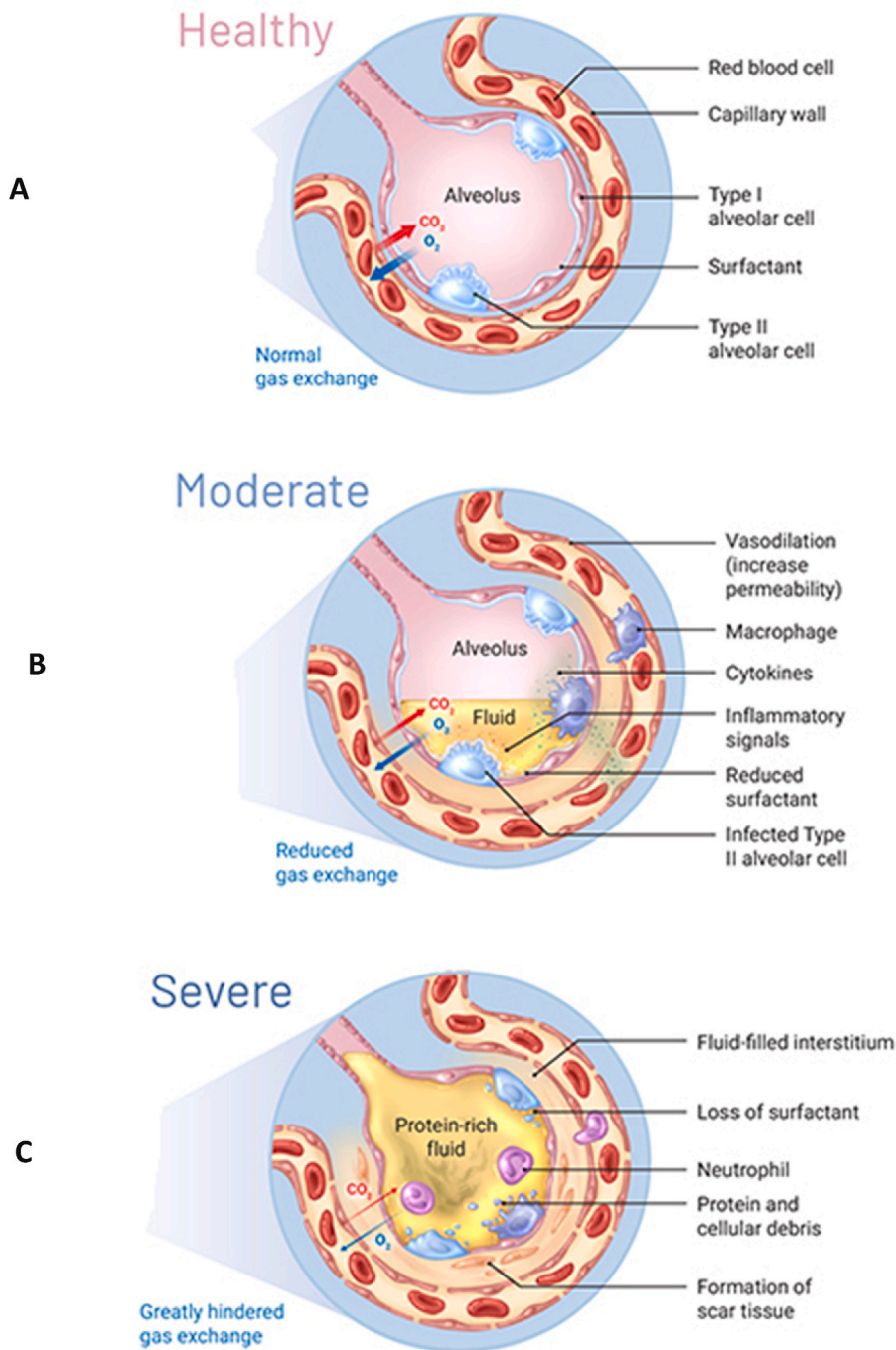| Parameters	value	Parameters	value
E_{alv}	$5\ cmH_2OL^{-1}$	HB	$0.74\ cmH_2OL^{-1}$
E_{cw}	$4\ cmH_2OL^{-1}$	λ	$1.5 cmH_2O$
R_{ua}	$5\ cmH_2OL^{-1}$	μ	$1\ cmH_2O$
R_{ca}	$1\ cmH_2OL^{-1}$	a	-0.8
V_{tho}	$2L^{-1}$	b	-3

Fig. 4. Model of an infected alveolus in the lung. Type I and type II pneumocytes make up the alveolar walls and resident alveolar macrophages and pulmonary surfactant exist in the airspace (A). In the acute phase of SARS-CoV infection (B), type I and type II pneumocytes are infected and secrete inflammatory cytokines, while surfactant levels decrease. During the late stage/tissue damage portion of viral infection, viral titers decrease, while airway debris, pulmonary oedema and hyaline membrane formation impede respiration (C) [31].

α to control the alveolar volume (V_{alv}). Since COVID-19 increases the respiratory pattern, we insert a new parameter β in the Liénard systems [23] to control the frequency of respiration for patient subjected to coronavirus. Therefore, the dynamical equations (12) and (16) become, respectively:

$$\begin{cases} \dfrac{dx}{dt} = \beta\left[\left(ay^2 - by\right)x + \left(ay^3 + by^2\right) - HB\dfrac{dV_{alv}}{dt}\right] \\ \qquad\qquad \dfrac{dy}{dt} = \beta x \end{cases} \qquad\qquad 20$$

$$V_{th} = V_{\text{bth}} + \alpha V_{\text{alv}} \qquad\qquad 21$$

Because the work of breathing increases the respiratory pattern during the respiration for a patient subjected to COVID-19, this affects the pleural pressure which has a considerable effect on the pulmonary vascular resistance due to ventilation [30]. carried out experimental works in which they measured systemic and pulmonary artery pressures, pleural pressure and flow rates during mechanical ventilation. If the respiratory drive has been suppressed, it can be assumed that thoracic compliance remains constant during ventilation. Under these conditions and according to Ref. [8]; the lung volume, the pleural pressure and the pulmonary vascular resistance should all vary proportionally one another. Therefore, during the mechanical inspiration, pulmonary vascular resistance will increase as pleural pressure grows and vice versa. Under such conditions, the model of [33] defined by $R_p(t) = C_R P_l(t)$ could not be sufficient to explain such quick and fast development of the virus (Fig. 5). Therefore, to couple robustly the effect of COVID-19 to the respiratory system, we propose an exponential relationship between the pleural pressure and the pulmonary cavity resistance as follows:

$$R_p(t) = C_R \, exp(P_l(t)) + R_{p,0} \qquad\qquad 22$$

In Eq. (22), the quantity C_R represents the gain of the relationship between the pleural pressure and the pulmonary resistance and it is equal to $7 \times 10^3 Kpa.s.m^{-3}$ [33]. Before continuing, we recall that [33] proposed a model of pulmonary resistance for a patient placed on assisted ventilation. Then, they showed that this resistance is a function of pleural pressure and increases with each breath. In our
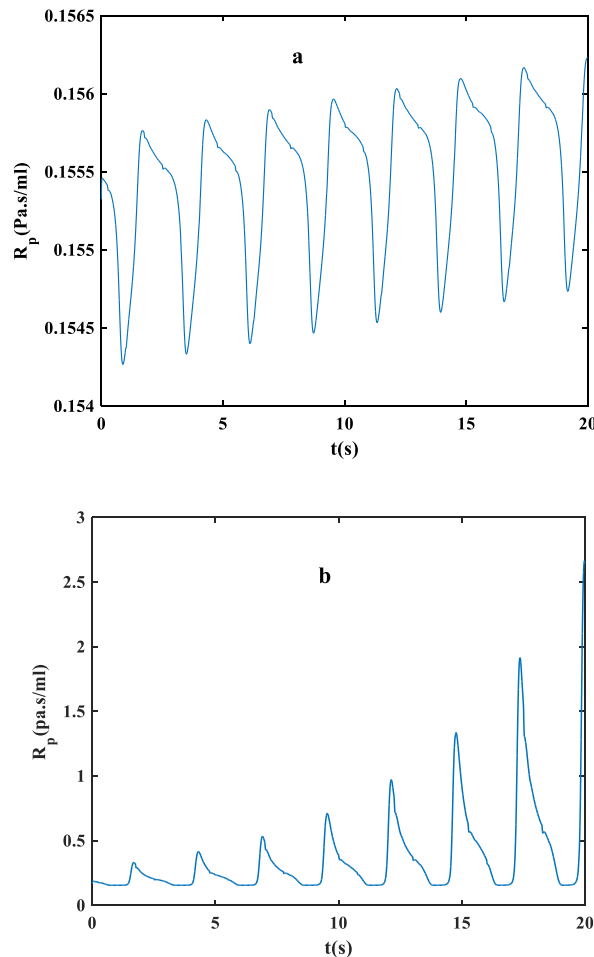

Fig. 5. Temporal evolution of the lung resistance with each breath (a) model of [33] (b) our proposed model defined by Eq. (22). These plots display the increase in pulmonary resistance with each breath. It appears that growth in Smith's model (case a) is not as fast as in our model (case b). In (b) case, the lung resistance is greater.

case, we propose a model that grows faster due to the swelling of the respiratory alveoli, leading to an increase in lung resistance. Considering the covid-19 situation, we compare the two models of lung resistance (Fig. 5). These plots exhibit the increase in pulmonary resistance with each breath. However, it appears that growth in Smith's model (Fig. 5a) is not as fast as in our model (Fig. 5b). These results make it possible to understand that in a pathological situation, Smith's model would not capture the rapid dynamics of virus development. Therefore, we believe that with proper calibration, our model could encapsulate these dynamics.

Now, we investigate the effects of COVID-19 which could be considered in the model in two ways: (**i**) by increasing the alveoli volume controlled with the parameter α (Eq. (21)) and (**ii**) by modifying the constant pulmonary resistance through the insertion of the time varying model (Eq. (22)) as function of the pleural pressure.
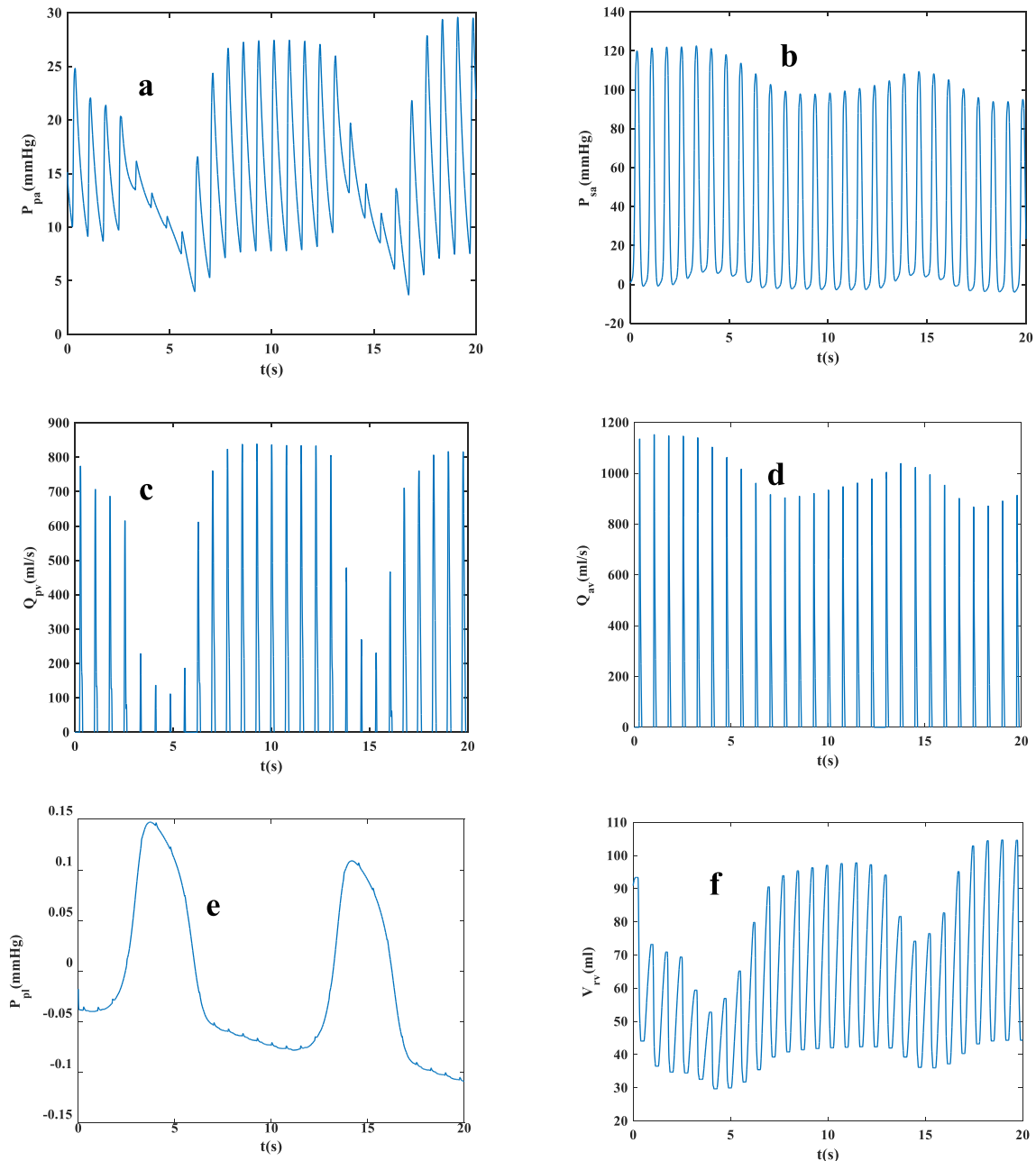

Fig. 6. Cardiopulmonary system model: simulations of the mechanical ventilation with constant pulmonary vascular resistance ($R_p = 0.1552 Kpa.s.mL^{-1}$) exhibiting the temporal evolution of: (a) pressure in pulmonary artery; (b) pressure in systemic artery; (c) Flow rate in the pulmonary vein; (d) Flow in systemic artery; (e) Pleural pressure and (f) Volume of the right ventricle. We recover the results established by Ref. [33].

3. Results and discussion

3.1. Model validation

In this subsection, we intend to examine the dynamics of the cardiopulmonary model for constant pulmonary vascular resistance (R_p) which is described by the following two sets of equations: one for the circular system (Eqs. (1)–6)) and the second set for the respiratory system (Eqs.(12)–17)). The sets of equations (1) and (1)–(6)2-17) are integrated numerically through the fourth order Runge-Kutta method and the results are displayed in Fig. 6 for the parameters defined in Tables 1–4 The simulated flow in pulmonary valve (Q_{pv}), the value of pleural pressure (Fig. 6e), the value of the pressure in systemic artery (Fig. 6b) and the pressure in pulmonary artery (Fig. 6a) corroborates the simulation results established by Ref. [33]. Likewise, the simulated flows in aortic valve (Q_{av}) are also similar to those obtained for the flows in aortic valve (Q_{av}) by Ref. [33].

We numerically integrate the two sets of equations (1) and (1)–(6)2-17) over 25 cardiac cycles and observe the temporal variation of the amplitude of each characteristic parameter in each cycle: reduction or increment can be observed depending on the chosen case. We have also observed numerically the effects of the respiratory system on the vascular system during several cardiac cycles and therefore, the obtained results should be analyzed in a global way. Indeed, the reduction of the flow (Q_{pv}) in pulmonary artery (Fig. 6c) is due to the increase in pleural pressure during inspiration. This compresses the heart and reduces the filling of the right ventricle (V_{rv}) which was initially at $95ml$ at the first cycle (Fig. 6f) and thus immediately reduces the flow through the pulmonary artery. This effect is reversed on exhalation, when the flow in the pulmonary artery quickly returns to its initial value. The reduction in the systemic artery flow (Q_{av}) (Fig. 6d) is slightly delayed (as seen in Fig. 6c and d, respectively, the amplitude of Q_{pv} falls directly when Q_{av} lies its amplitude over 4 cycles before falling which creates a delay between the two flows) compared to the reduction in Q_{pv}, because the increase in pleural pressure actually causes a slight growth in the systemic artery flow when blood is expelled from the pulmonary circulation. However, this increment is quickly overcome by the reduction in blood flow due to the restriction of pulmonary perfusion and the decrease in pulmonary filling (Q_{pv}). The flow in the aorta begins to augment again during expiration. However, Fig. 6 shows that there is a delay between the onset of expiration and the start of the increase in flow.
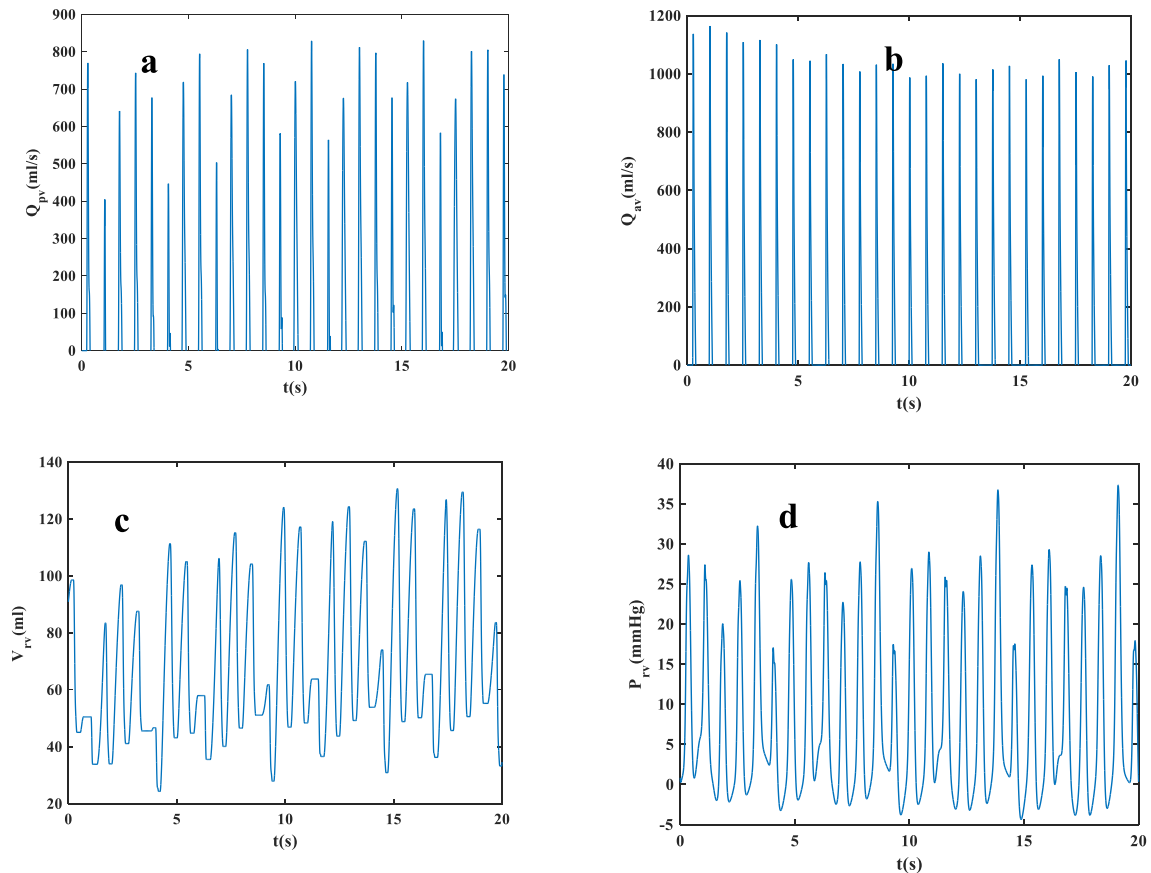

Fig. 7. Effect of the high frequency induced by covid-19 ($\beta = 2$), augmentation of the frequency due to the lung disease: (a) flow in the pulmonary artery; (b) systemic artery flow; (c) right ventricle volume; (d) right ventricle pressure.

3.2. Effects of high frequency induced by covid-19 on the cardiopulmonary system

In this subsection, we investigate the effects of high frequency induced by the coronavirus-19 on the dynamics of the cardiopulmonary system. The sets of equations describing the dynamics of the model are given by Eqs. (1)–(1)–(6)(1)–(6) and Eqs.12–17. Here, the pulmonary vascular resistance (R_p) is still constant but the parameters β (from Eq. (20)) varies in order to simulate the high frequency respiration. The results of the numerical simulation of our proposed mathematical model are displayed in Fig. 7. These numerical outcomes are in perfect agreement with some conclusions carry out by the clinicians in our reference hospitals (General Hospital of Yaoundé and La Quintiniae Hospital of Douala [21]).
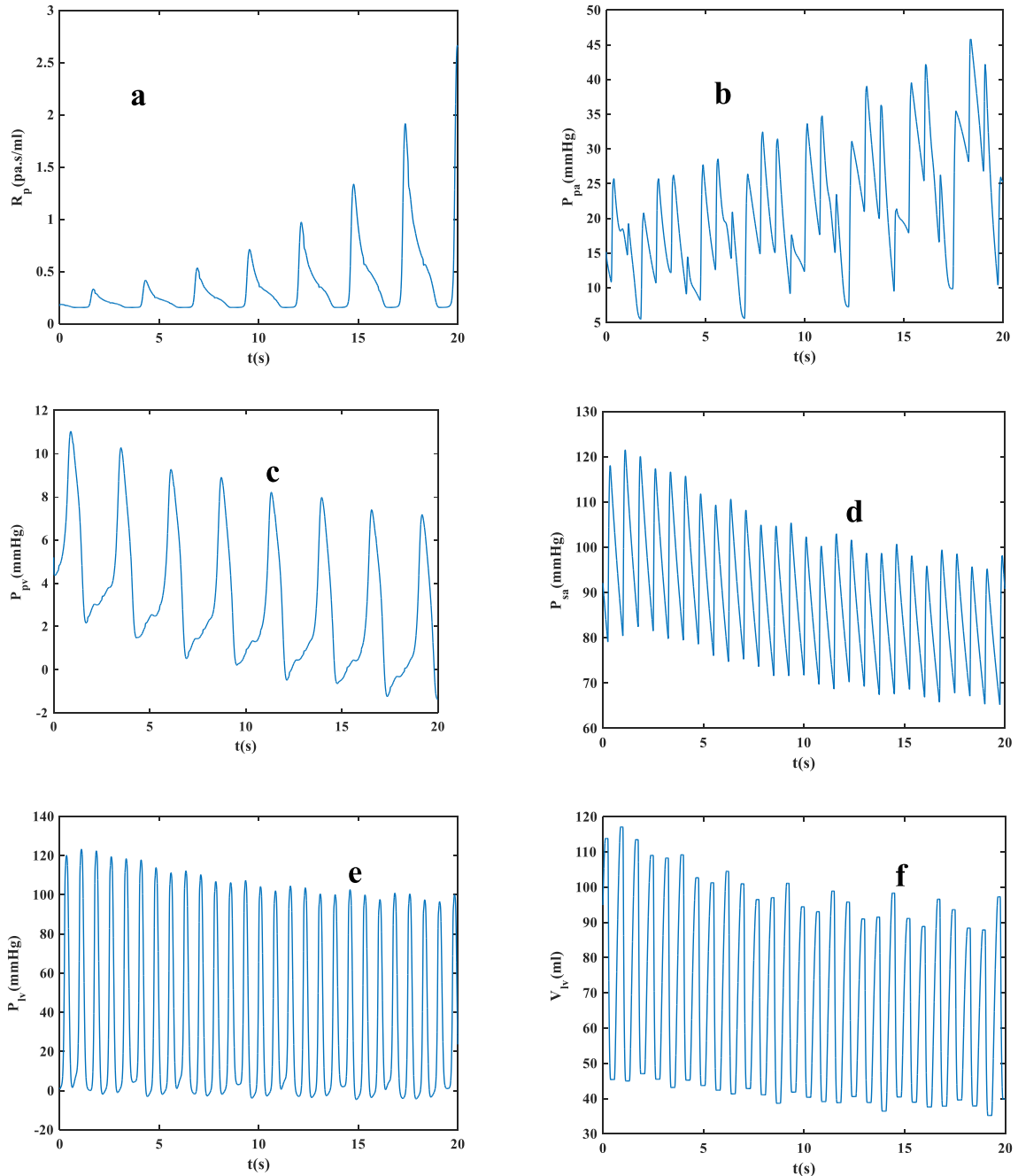

Fig. 8. Effect of the time varying pulmonary resistance $R_p(t)$ on the vascular circulation with the value of $C_r = 7 \times 10^3 Kpa.s.m^{-3}$: (a) pulmonary resistance; (b) pressure in pulmonary atery; (c) pressure in the pulmonary vein; (d) pressure in systemic atery; (e) pressure of left ventricle; (f) volume of left ventricle.

It was shown that patients with suspected cardiovascular disease were at increased risk of severe case if they had covid-19 [7]. To understand this, the focus was initially done on the respiratory rhythm. Patients with covid-19 were oxygen-deprived and had difficulty breathing, most had symptoms of severe lung disease [7]. The patients we have the opportunity to see had an elevated respiratory rate [3]. To simulate this situation, we boost the respiratory rate by assuming that a patient with covid-19 possesses a respiratory rate twice the normal rate (that is, $\beta = 2$). It appears that the flow in the pulmonary artery (Q_{pv}) (Fig. 7a) grows and diminishes spontaneously due to the respiratory rate during expiration and inspiration. This has the immediate effect of decreasing the filling of the right ventricle (V_{rv}) as observed in Fig. 7c. It is also constant that this augmentation of frequency causes the right ventricle to fill and partially release (V_{rv}), which results in an intermittent variation of the pressure (P_{rv}) in the ventricle (Fig. 7d). This action reduces the efficiency of the cardiac pump, and could justify the fact that a patient with cardiovascular disease appears to be more vulnerable to covid-19 [7].

As the cardiac muscle increases and decreases by the intermittent variation of the pressure, this situation could cause myocardial injury which is significantly associated with fatal outcome of covid-19, while the prognosis of patients with underlying cardiovascular diseases but without myocardial injury is relatively favorable due to this effect of pressure variations. Myocardial injury is associated with cardiac dysfunction and arrhythmias [13]. Inflammation may be a potential mechanism for myocardial injury [13]. Aggressive treatment may be considered for patients at high risk of myocardial injury [13]. When the frequency grows, the delay between the systemic artery flow (Q_{av}) (Fig. 7b) and the flow in the pulmonary artery (Q_{pv}) is reduced because the pleural pressure that causes a slight increment in the systemic artery flow is accelerated by the respiratory rate. These results show that a patient with a myocardial inflammatory disease is exposed to a severe case of inflammation if he/she has covid-19. Similarly, patients with covid-19 without medical history of cardiovascular disease are likely to have a myocardial injury because of this intermittent high rhythm of breathing. This lesion or injury is due to the high respiratory rate and the angiotensin converting enzyme 2.

3.3. Effects of the time varying pulmonary resistance

In this subsection, we will evaluate the impact of time varying pulmonary resistance on the dynamics of the cardiopulmonary system. Indeed, let us stress that the pulmonary resistance represents one of the main link between the cardiovascular system and the pulmonary system. Based on the fact that a patient with Covid19 starts noting but the modification of its alveoli volume, it is important to begin by checking the effects of this modification on the pulmonary resistance. Indeed, Fig. 8 that exhibit our simulation results shows the impact of varying the alveoli volume on the pleural pressure and therefore on the pulmonary resistance. These results display that variations of the alveoli volume provokes the increase of the pleural pressure of vascular cavities that induces the exponential growth of the pulmonary resistance.

As the respiratory alveoli enlarge due to the number of dead cells in them (alveoli) for a patient with covid-19, we simulate this effect by increasing the volume of the alveoli. We found that pleural pressure increases as the volume of the alveoli grows.

To better understand what happens in the vascular cavities, we introduce a new variable pulmonary resistance (R_p) with an exponential form to take into account the breathing difficulties due to the alveoli volume growth which increases the pulmonary resistance with each breath. As related experimental results do not yet exist, the most appropriate mathematical tool that could almost faithfully reproduce the expected physiological behavior of the model is an exponential function.

After numerical simulations, we observe in Fig. 8a that the growth in pleural pressure induces the increment of the pulmonary resistance (R_p) which decreases the flow in the pulmonary vein. This reduction in flow increases the pressure in the pulmonary artery (Fig. 8b) and causes a decrease in pressure in the pulmonary vein (Fig. 8c). Although the stroke volume diminishes during inspiration and augments during exhalation as it should normally be, there is a decrement in stroke volume (V_{lv}) in left heart (Fig. 8f) due to the diminution in flow in the pulmonary cavity. The decreasing pressure (P_{lv}) in the left ventricle (Fig. 8e) causes a stress in some organs and relieves others such as the systemic artery. Therefore, the pressure (P_{Sa}) in this cavity is reduced (Fig. 8d). This stress can indeed cause inflammation in the pulmonary artery. The growth of pressure in some organs and the reduction in pressure in others sufficiently prove the fact that covid-19 sufferers have a malfunction of the cardiac pump which can no longer pump blood properly and presents injury in the vascular cavities.

4. Conclusion

In this paper, we proposed a cardiopulmonary model to examine the impact of COVID-19 in the vascular system made of six-compartments including the systemic circulation and the pulmonary circulation. This cardiopulmonary model is constituted of a cardiovascular system coupled to the respiratory system. Based on the lumped parameters method, the dynamic of our model is checked. To consider the respiratory system and its frequency, we used a two-variable Liénard system and introduced a dynamical pleural pressure in the vascular system. This modeling allowed us to operate on certain system parameters to simulate the case of patients with COVID-19. We notably modified the volume of the respiratory alveoli, the frequency of the respiratory system and the pulmonary resistance. The fourth-order Runge-kutta algorithm is called for solving the motion equations. Our proposed model is validated by showing that the established outcomes for constant pulmonary resistance corroborate well the existing results [*IFAC Proceedings Volumes*, 39 (2006) 453–458]. Then we build a new exponential law for the time varying of the pulmonary resistance to better explain the cardiopulmonary system behavior for person with covid-19. The simulation results displayed that when the respiratory frequency grows, the delay between the systemic artery flow and the flow in the pulmonary artery decreases, inducing the reduction of the efficiency of the cardiac pump. It appeared that the growth of the alveoli volume provokes the increment of the pleural pressure in the vascular cavities that yields an exponential growth of the pulmonary resistance. Moreover, our results exhibited that the

augmentation of this pulmonary resistance is responsible of the growth of pressure in some organs and its diminution in others. Furthermore, we established that patients with covid-19 having a prior history of cardiovascular diseases are exposed to a severe case of inflammation/damage of their organs than those with no history of cardiovascular diseases. The proposed model could be exploited for implementation in a diagnostic medical tool where it is useful to simulate the changing effects in respiratory pressures in a patient's circulation system. It can also be used to build an overview on the effects of COVID-19 on the circulatory and respiratory systems. In the future work, we intend to conduct experiment whose outcomes will corroborate the theoretical results established within this paper. Furthermore, our cardiopulmonary model could be used to investigate the cumulative effects of high frequency with varying respiratory alveolar volumes for given clinical data.

Author contribution statement

R T Djoumessi: Conceived and designed the experiments; Performed the experiments; Analyzed and interpreted the data; Contributed reagents, materials, analysis tools or data; Wrote the paper.

V I P Dongmo; T J S Tadjonang: Performed the experiments; Analyzed and interpreted the data; Contributed reagents, materials, analysis tools or data; Wrote the paper.

François B PELAP: Conceived and designed the experiments; Analyzed and interpreted the data; Contributed reagents, materials, analysis tools or data; Wrote the paper.

Funding statement

Data availability statement

Data included in article/supp. Material/referenced in article.

Declaration of interest's statement

The authors declare no competing interests.

Ethical approval

Not required.

Appendix A. Supplementary data

Supplementary data related to this article can be found at https://doi.org/10.1016/j.heliyon.2023.e12908.

References

[1] A. Aksenov, S. Zhluktov, W. Zietak, R. Cotton, D. Vucinic, Human heart blood flow numerical modelling and simulations, in: Advances in Visualization and Optimization Techniques for Multidisciplinary Research, Springer, Singapore, 2020, pp. 237–263.

[2] A. Albanese, L. Cheng, M. Ursino, N.W. Chbat, An integrated mathematical model of the human cardiopulmonary system: model development, Am. J. Physiol. Heart Circ. Physiol. 310 (7) (2016) H899–H921.

[3] M. Bansal, Cardiovascular disease and COVID-19, Diabetes Metabol. Syndr.: Clin. Res. Rev. 14 (3) (2020) 247–250.

[4] J.O. Campos, J. Sundnes, R.W. Dos Santos, B.M. Rocha, Effects of left ventricle wall thickness uncertainties on cardiac mechanics, Biomech. Model. Mechanobiol. 18 (5) (2019) 1415–1427.

[5] D.C. Chung, S.C. Niranjan, J.W. Clark Jr., A. Bidani, W.E. Johnston, J.B. Zwischenberger, D.L. Traber, A dynamical model of ventricular interaction and pericardial influence, Am. J. Physiol. Heart Circ. Physiol. 272 (1997) H2942–H2962.

[6] F.J. Clark, C. Von Euler, On the regulation of depth and rate of breathing, J. Physiol. 222 (1972) 267–295.

[7] K.J. Clerkin, J.A. Fried, J. Raikhelkar, G. Sayer, J.M. Griffin, A. Masoumi, S.S. Jain, D. Burkhoff, D. Kumaraiah, L. Rabbani, A. Schwartz, COVID-19 and cardiovascular disease, Circle 141 (20) (2020) 1648–1655.

[8] E. D'Angelo, M. Pecchiari, P.D. Valle, A. Koutsoukou, J. Milic-Emili, Effects of mechanical ventilation at low lung volume on respiratory mechanics and nitric oxide exhalation in normal rabbits, J. Appl. Physiol. 99 (2) (2005) 433–444.

[9] A. Davidovic, Y. Coudiere, Y. Bourgault, Modelling the action potential propagation in a heart with structural heterogeneities: from high resolution MRI to numerical simulations, Int. J. Numer. Methods Biomed. Eng. (2020) e3322, https://doi.org/10.1002/cnm.3322.

[10] F.L. Ellwein, J. Khoury, R.R. Moores Jr., L. Linkous, M. Brandes, H.J. Rozycki, Theoretical open-loop model of respiratory mechanics in the extremely preterm infant, PLoS One 13 (6) (2018), e0198425, https://doi.org/10.1371/journal.pone.0198425.

[11] J.J. Fontecave, E. Abdulhay, P. Calabrese, P. Baconnier, P.Y. Gumery, A model of mechanical interactions between heart and lungs, Phil. Trans. Roy. Soc. A 367 (1908) (2009) 4741–4757.

[12] J.J. Fontecave, P. Baconnier, A simple mathematical model of spontaneous swallow effects on breathing based on new experimental data, in: 2016 38th Annual International Conference of the IEEE Engineering in Medicine and Biology Society, EMBC), August 2016, pp. 4260–4263.

[13] N.G. Frangogiannis, The inflammatory response in myocardial injury, repair, and remodelling, Nat. Rev. Cardiol. 11 (5) (2014) 255–265.

[14] S.V. Frolov, S.V. Sindeev, V.A. Lischouk, D.S. Gazizova, D. Liepsch, A. Balasso, A lumped parameter model of cardiovascular system with pulsating heart for diagnostic studies, J. Mech. Med. Biol. 17 (3) (2017), 1750056.

[15] T. Guo, Y. Fan, Y. Chen, X. Wu, L. Zhang, T. He, H. Wang, J. Wan, X. Wang, Z. Lu, Cardiovascular implications of fatal outcomes of patients with coronavirus disease 2019 (COVID-19), JAMA cardiology 5 (7) (2020) 811–818.

[16] K. Hemalatha, M. Manivannan, A study of cardiopulmonary interaction haemodynamics with detailed lumped parameter model, Int. J. Biomed. Eng. Technol. 6 (3) (2011) 251–271.

[17] E. Jung, C.F. Babbs, S. Lenhart, V.A. Protopopescu, Optimal strategy for cardiopulmonary resuscitation with continuous chest compression, Acad. Emerg. Med. 13 (7) (2006) 715–721.

[18] C.H. Kim, K.S. Song, N.A. Trayanova, K.M. Lim, Computational prediction of the effects of the intra-aortic balloon pump on heart failure with valvular regurgitation using a 3D cardiac electromechanical model, Med. Biol. Eng. Comput. 56 (5) (2018) 853–863.

[19] C.K. Knox, Characteristics of inflation and deflation reflexes during expiration of the cat, J. Neurophysiol. 36 (1973) 284–295.

[20] I. Kokalari, T. Karaja, M. Guerrisi, Review on lumped parameter method for modeling the blood flow in systemic arteries, J. Biomed. Sci. Eng. 6 (1) (2013), 27458, https://doi.org/10.4236/jbise.2013.61012.

[21] L.M. Kuate, W. Ngatchou, M.N. Temgoua, C. Kouanfack, D. Lemogoum, J.N. Tochie, J.T. Sobngwi, Electrocardiographic safety of daily Hydroxychloroquine 400mg plus Azithromycin 250mg as an ambulatory treatment for COVID-19 patients in Cameroon, medRxiv 11 (2) (2021), https://doi.org/10.4236/wjcd.2021.112012.

[22] C. Leguy, Mathematical and computational modelling of blood pressure and flow, in: Cardiovascular Computing-Methodologies and Clinical Applications, Springer, Singapore, 2019, pp. 231–246.

[23] A. Lienard, Etude des oscillations entretenues, Revue Générale de l'Electricité 23 (1928) 901–912, 946-954.

[24] K. Lu, J.R. Clark, F.H. Ghorbel, D.L. Ware, W. Bidani, A human cardiopulmonary system model applied to the analysis of the Vasalva maneuver, Am. J. Physiol. Heart Circ. Physiol. 281 (2001) H261–H2679.

[25] Montebelli, G. Effects of Expiratory Flow Limitation on Mechanical Cardio-Pulmonary Interactions: a Model Study. PhD thesis, Politecnico di Milano 2005, 166p.

[26] S.A. Niederer, K.S. Campbell, S.G. Campbell, A short history of the development of mathematical models of cardiac mechanics, J. Mol. Cell. Cardiol. 127 (2019) 11–19.

[27] J.T. Ottesen, M.S. Olufsen, J.K. Larsen, Applied mathematical models in human physiology, Society for Industrial and Applied Mathematics 33 (5) (2004) 719, https://doi.org/10.1007/s10439-005-4399-6.

[28] A. Propp, A. Gizzi, F. Levrero-Florencio, R. Ruiz-Baier, An orthotropic electro-viscoelastic model for the heart with stress-assisted diffusion, Biomech. Model. Mechanobiol. 19 (2) (2020) 633–659.

[29] V. Rolle Le, N. Samson, J.P. Praud, A.I. Hernandez, Mathematical modeling of respiratory system mechanics in the new born lamb, Acta Biotheor. 61 (1) (2013) 91–107.

[30] S.M. Scharf, R. Brown, N. Saunders, L.H. Green, Hemodynamic effects of positive-pressure inflation, J. Appl. Physiol. 49 (1) (1980) 124–131.

[31] N. Singh, B. Suthar, A. Mehta, N. Nema, A. Pandey, Corona virus : an immunological perspective review, Int. J. Immunol. Immunother 7 (1) (2020) 50, https://doi.org/10.23937/2378-3672/1410050.

[32] B.W. Smith, S. Andreassen, G.M. Shaw, P.L. Jensen, S.E. Rees, J.G. Chase, Simulation of cardiovascular diseases by including the autonomic nervous system into a minimal model, Comput. Methods Progr. Biomed. 86 (2007) 153–160.

[33] B.W. Smith, S. Andreassen, G.M. Shaw, S.E. Rees, J.G. Chase, Cardiovascular system modelling of heart-lung interaction during mechanical ventilation, IFAC Proc. Vol. 39 (18) (2006) 453–458.

[34] K. Sunagawa, K. Sagawa, W.L. Maughan, Relations de volume de pression ventriculaire end-systolique, in: The Ventricle, Springer, Boston, MA, 1985, pp. 79–103.

[35] H. Talbot, F. Spadoni, C. Duriez, M. Sermesant, M. O'Neill, P. Jais, H. Delingette, Interactive training system for interventional electrocardiology procedures, Med. Image Anal. 35 (2017) 225–237.

[36] J. Wagner, P. Agostoni, R. Arena, R. Belardinelli, D. Dumitrescu, A. Hager, A. Schmidt-Trucksass, The role of gas exchange variables in cardiopulmonary exercise testing for risk stratification and management of heart failure with reduced ejection fraction, Am. Heart J. 202 (2018) 116–126.

[37] N. Westerhof, J.W. Lankhaar, B.E. Westerhof, The arterial windkessel, Med. Biol. Eng. Comput. 47 (2) (2009) 131–141.